medRxiv preprint doi: https://doi.org/10.1101/2023.08.06.23293535; this version posted August 9, 2023. The copyright holder for this preprint (which was not certified by peer review) is the author/funder, who has granted medRxiv a license to display the preprint in perpetuity. It is made available under a CC-BY-NC-ND 4.0 International license .

Identification of anatomical and angio-architectural features of at-risk cranial dural arteriovenous fistulas using machine learning approaches.

Katharina Frank[1,3], Paiman Shalchian-Tehran[1,3], Mihai Manu[1,3*], Zafer Cinibulak[1] , Jörg Poggenborg[2], Makoto Nakamura[1]

[1.]Department of Neurosurgery, Cologne-Merheim Medical Center, Witten/Herdecke University
[2.]Department of diagnostic and interventional Radiology and Neuroradiology, Cologne-Merheim Medical Center, Witten/Herdecke University
[3.] these authors contributed equally
* corresponding author mihai.manu@uni-wh.de

Background. Cranial dural arteriovenous fistulas (dAVF) are rare complex vascular malformations that have a bleeding risk with potential lethal consequences. Despite this, knowledge of the vascular architectural features associated with the rupture risk are not always clearly defined.
Methods. We retrospectively analyzed cranial arteriovenous fistulas in terms of their anatomical and angio-architectural features as evaluated on conventional subtraction angiography: Location of the fistula, fistula architecture, venous ectasia or pouches, presence of cortical draining veins, presence of pial feeders, outflow stenosis, presence of a major sinus thrombosis, flow-associated arterial aneurysms as well as presenting symptoms. Patterns in the data were identified after multiple components analysis followed by automatic k-means clustering and their predictive power was confirmed using a shallow feedforward neural network.
Results. New relevant features predictive of hemorrhage, identified by using a shallow feed-forward neural network, were outflow stenosis, in addition to venous cortical drainage and venous ectasia. The neural network achieved relatively high performance metric, with area under the receiver operating characteristic curve (ROC AUC)) of 0.88 and accuracy of 0.8. We confirmed the relevance of these findings by performing a multiple correspondence analysis followed by k-means clustering in the angiographic feature vector space, additionally identifying architecture of the fistula as relevant factor. There was good agreement between the ground truth (hemorrhage) and the cluster labels (adjusted Rand score 0.273, purity index 0.82).
Conclusion. Machine learning approach confirmed the importance of previously described features (cortical drainage and venous ectasia) but also uncovered novel relevant characters (outflow stenosis and fistula architecture) for the hemorrhage risk.

Introduction

Cranial dural arteriovenous fistulas (dAVF) are abnormal direct arteriovenous shunts within the dura with multifactorial pathogenesis, which are acquired and can develop spontaneously, after traumatic head injury or e.g. after thrombosis of the venous sinus.

NOTE: This preprint reports new research that has not been certified by peer review and should not be used to guide clinical practice.

medRxiv preprint doi: https://doi.org/10.1101/2023.08.06.23293535; this version posted August 9, 2023. The copyright holder for this preprint
(which was not certified by peer review) is the author/funder, who has granted medRxiv a license to display the preprint in perpetuity.
It is made available under a CC-BY-NC-ND 4.0 International license .

dAVFs are making up around 10% of all intracranial vascular malformations and have an incidence around 0,15-0,29 per 100,000 adults per year(1, 2). Patients harboring these malformations are typically middle-aged, but the lesions can, although less frequently, occur in children. The symptoms are presumed to depend on the presence or absence of venous hypertension and can vary from benign (tinnitus) up to severe hemorrhage in any of the three compartments (intracerebral, subdural and/or subarachnoidal) or non-hemorrhagic neurologic deficits (NHNDs) such as seizures(2). Regardless of presentation, the first line imaging tools are computed tomography and CT-angiography, less frequently magnetic resonance imaging/angiography/venography (MRI, MRA, MRV), whereas digital subtraction angiography (DSA) represents the gold standard for diagnosis and therapy(3).

There are several classification and grading systems, aiming to stratify the risk and guide treatment decisions, of which the Cognard and the Borden classifications are commonly used(4, 5). Higher-grade fistulas, associated with venous hypertension and consequently ectatic cortical veins, are presumed to carry an increased hemorrhage risk, have poorer outcomes and thus are prone to a more aggressive treatment approach(6-8).

We hypothesized that venous hypertension is the result of nonlinear interactions of features that have a direct angiographic correspondence (not necessarily in the form of dilated cortical veins, as evidenced by symptomatic fistulas that do not exhibit this character), that the hemorrhage risk of dAVF may largely depend on these features, and that these dependencies, given their nonlinear nature, are not likely captured by traditional statistical methods. Our goal was to explore the use of machine learning in identifying potential relevant, hidden, angio-architectural features of dural arteriovenous fistulas helping neurosurgeons and interventional neuroradiologists in clinical decision-making process.

Methods

Our retrospective cohort comprised 23 cranial dural arteriovenous fistulas that underwent digital subtraction angiography at the Department of Neurosurgery of the Cologne-Merheim Medical Center between January 2017 and December 2022. Additionally, all patients that presented with hemorrhage or non-hemorrhagic neurological deficits received at least a CT scan or CT-angiography. The recorded imaging parameters were location of the fistula, fistula architecture, venous ectasia, cortical venous drainage, presence of pial feeders, outflow stenosis, presence of a major sinus thrombosis and flow-associated arterial aneurysms. The clinical variables included age, sex and symptoms at presentation.

The machine learning was implemented by means of custom-written routines in Python. We applied a dimensionality reduction algorithm (multiple correspondence analysis (MCA), prince python package (9)) to identify the direction of largest variance by performing a singular value decomposition of the chi-square distance matrix

medRxiv preprint doi: https://doi.org/10.1101/2023.08.06.23293535; this version posted August 9, 2023. The copyright holder for this preprint (which was not certified by peer review) is the author/funder, who has granted medRxiv a license to display the preprint in perpetuity. It is made available under a CC-BY-NC-ND 4.0 International license .

$\boldsymbol{D} = \boldsymbol{U} \cdot \boldsymbol{S} \cdot \boldsymbol{V}^T$, where the elements of $\boldsymbol{D}$ are given by $d_{ij} = \sqrt{\frac{(e_{ij} - x_{ij})^2}{e_{ij}}}$ (where e_{ij} and x_{ij} are the elements of the expected, respectively observed, frequency matrices), $\boldsymbol{U}$ and $\boldsymbol{V}$ are orthogonal matrices with columns representing the position of categories along the principal components and $\boldsymbol{S}$ is a diagonal matrix containing the singular values, representing the amount of variance explained by each principal component. For the automatic k-means clustering, the data is then divided into a number of clusters in trying to minimize the error function $E = \sum_{k=1}^{C} \sum_{x \in Q_k} \| x - c_k \|^2$, where x represents the data, C is the number of clusters, c_k is the center of cluster k and $\| \ldots \|$ denotes the Euclidean norm. The number of clusters is predefined by plotting the within cluster sum-of-squares (wcss) as a function of k and choosing the inflection point (elbow of the curve) as the number of clusters to use.

The neural network implementation was based on the multi-layer perceptron (MLP) classifier of the scikit-learn Python package(10). The shallow feedforward neural network had one output and one input layer as well one hidden layer comprising 12 neurons with rectified linear activation functions (ReLU) and standard backpropagation with gradient descent (Adam) with the goal to minimize the objective function (binary cross-entropy loss).

Results

The median age at the time of diagnosis was 59 years (range: 28-84). There were 70% males (16/23) and 30% female (7/23) patients. In terms of presenting symptoms, 39% (9/23) had an intracranial hemorrhage (Figure 1 B and F), 34% (8/23) complained of tinnitus, 13% (3/23) had seizures, 4% (1/23) had a visual field deficit, 8% (2/23) had unspecific symptoms such as dizziness or were asymptomatic. Most of the dAVF where of Cognard Grade IV (11/23, 47.8%), followed by Grade IIb (5/23, 21.7%), Grade III (4/23, 17.3%). Cognard Grade I, IIa and V made up 4% (1/23) each of the remaining dAVF in our series. The most common anatomical location of the fistulas was tentorial (7/23, 30%) followed by transverse sinus/ sigmoid sinus junction (6/23, 26%), convexity (5/23, 21%), petrosal (2/23, 8%), foramen magnum (2/23, 8%) and ethmoidal (1/23, 6%).

We characterized the fistula architecture based on the presence of single or multiple feeding arteries (single feeder vs multi-feeder) that either converged to a common point or spread out along the collecting vein. The majority of lesions were of the multiple feeder spread out type (14/23, 60%) (Figure 1 C), the rest of the fistula architecture being either converging multiple feeder (8/23, 36%) or single feeder/single point (4%, 1/23) type. Venous ectasia, defined as a cortical dilated vein of more that 5mm

medRxiv preprint doi: https://doi.org/10.1101/2023.08.06.23293535; this version posted August 9, 2023. The copyright holder for this preprint
(which was not certified by peer review) is the author/funder, who has granted medRxiv a license to display the preprint in perpetuity.
It is made available under a CC-BY-NC-ND 4.0 International license .

diameter, was demonstrated in 52% (12/23) (Figure 1 A and E). Outflow stenosis was considered in those cases where there was a 50% abrupt change in the diameter of the cortical draining vein (65%, 15/23) (Figure 1 A, D and E). Thrombosis of a major sinus was present in 26% (6/23) of the surveyed angiographies. Reflux in a cortical draining vein was found in 86% (20/23) of cases. 39% (9/23) of the dAVF exhibited pial feeding arteries, and of these, a third had a flow associated arterial aneurysm (Figure 1 D).

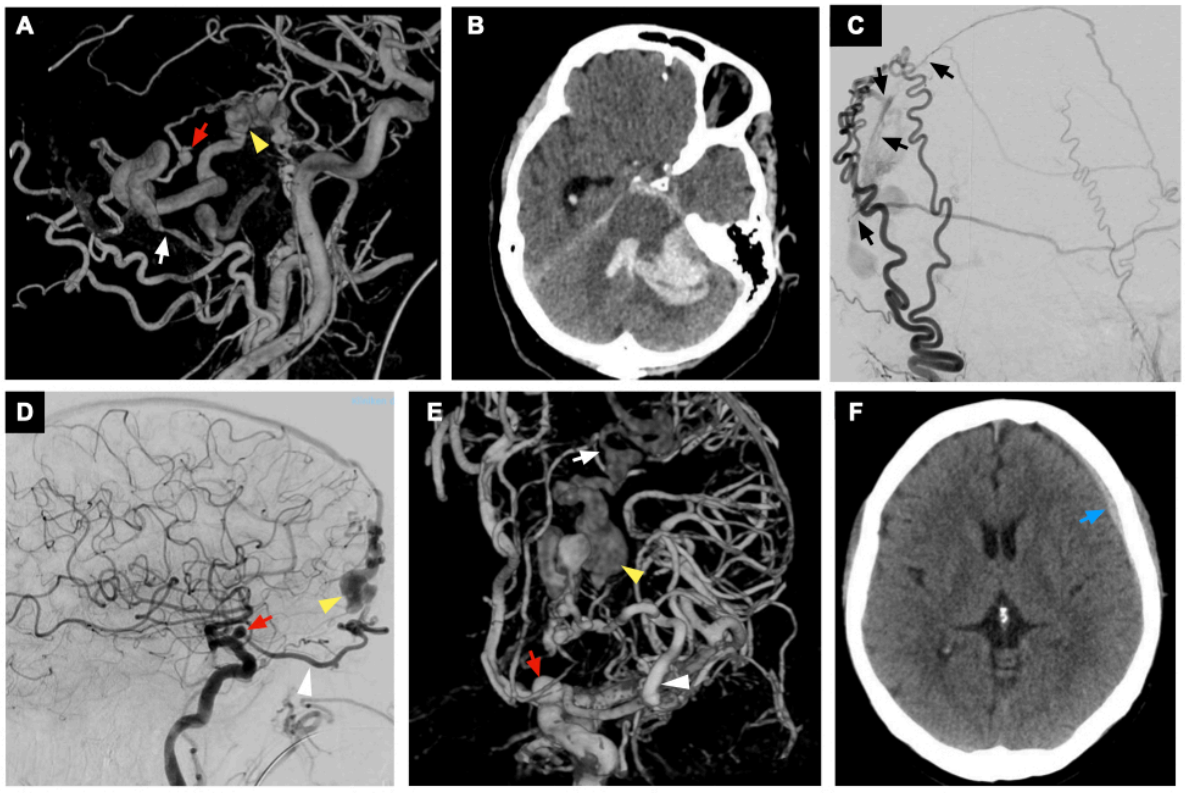

Figure 1. Angiographic characters of dural arteriovenous fistulas. (A) 3D reconstruction of a common carotid injection showing ectatic cortical veins (yellow arrowhead), segmental stenosis of the draining vein (white arrow) as well as an flow-associated aneurysm (red arrow). (B) Same patient as in A, CT scan showing cerebellar hemorrhage. (C) External carotid injection in another case showing a multiple feeder (black arrows) spread out type of fistula. (D) Left internal carotid injection showing a flow-associated aneurysm as well as dilated cortical vein (color coding as in A). Note the prominent ophthalmic artery (white arrowhead). (E) 3D reconstruction of the previous angiography, viewed anterograde, demonstrating additionally a segmental stenosis of the draining vein (white arrow, color coding as in A). (F) Same patient as in D and E, CT scan at presentation demonstrating a small left sided acute, non-traumatic subdural hematoma.

In order to extract hidden and relevant features for the hemorrhage risk from the conventional subtraction angiography, we trained (80% of the data) and tested (20% of the data) a shallow feed-forward neural network (ANN), where the input was a list of fistula characters and the output was the probability of being in one of two categories (hemorrhage vs non-hemorrhage, Figure 2 A). The model achieved a relatively high receiver operating characteristic area under the curve (ROC AUC) score of 0.88 and an

medRxiv preprint doi: https://doi.org/10.1101/2023.08.06.23293535; this version posted August 9, 2023. The copyright holder for this preprint
(which was not certified by peer review) is the author/funder, who has granted medRxiv a license to display the preprint in perpetuity.
It is made available under a CC-BY-NC-ND 4.0 International license .

accuracy of 0.8, indicating good performance in predicting the outcome of interest (Fig are 2 B). Independently checking the model performance with 5-fold cross-validation resulted in a cross-validation accuracy of 0.82 ± 0.094.

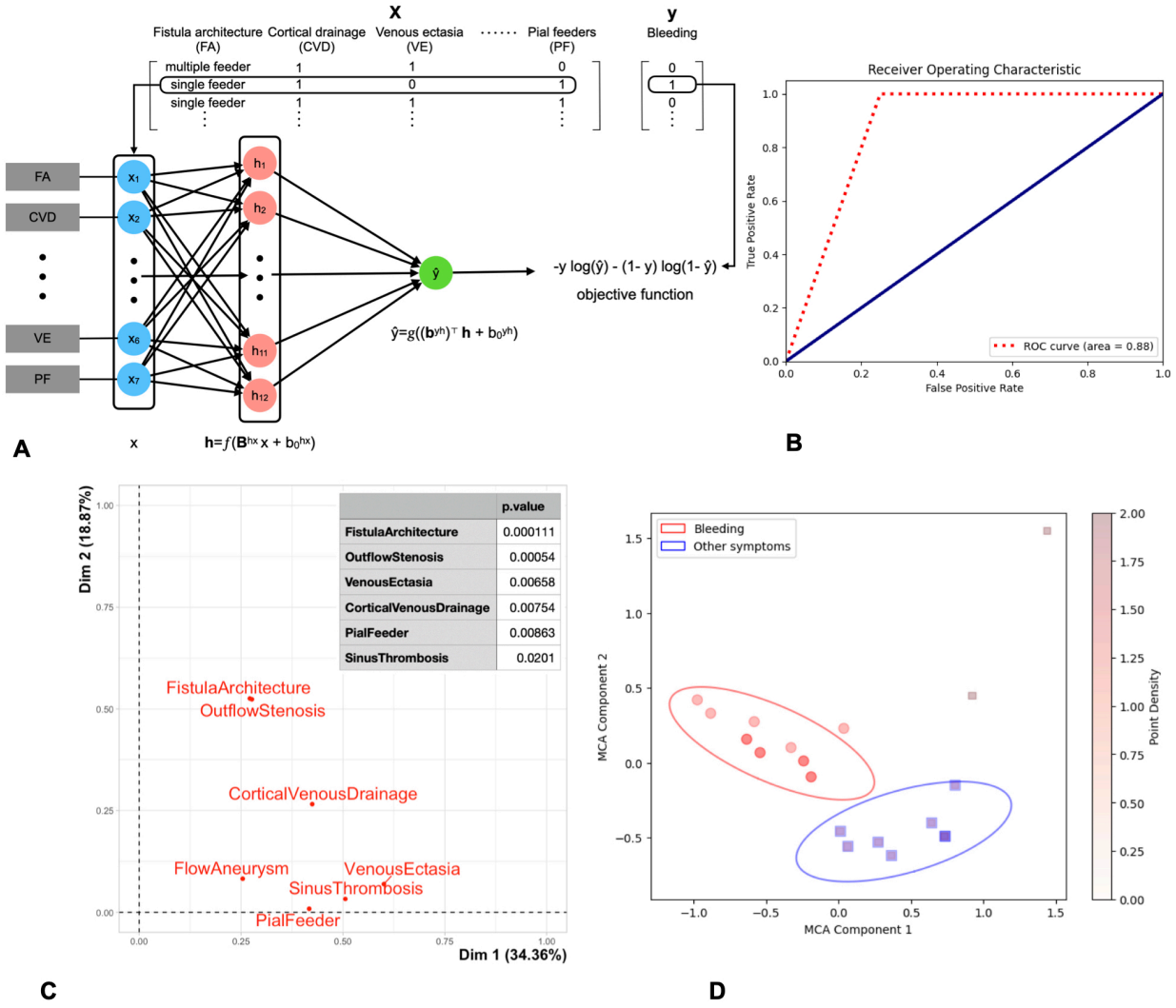

Figure 2. Machine learning classification and clustering of cranial dural arterio-venous fistulas. (A) Illustration of the shallow feed-forward neural network (multi-layer perceptron, MLP). The input layer (blue) takes a binary vector of the predictors (fistula characters, top) x, computes the h vector as a weighted sum of the input by multiplying with a weight matrix B and then passing the result through a ReLU function f. In the final stage, the output (green) is computed as a weighted sum of h passed through a sigmoid activation function g. The output value corresponds the probability of meeting the outcome criteria (bleeding, y). (B) Graphical representation of the MLP performance as area under the curve of the ROC. (C) Predictor variable representation after dimensionality reduction using multiple correspondence analysis (MCA) showing the correlation between the angiographic features and the principal dimensions. The individual coordinates are given by the squared correlations. Dim1 and 2 correspond to the first principal components and shown with their percentage of explained variance. Insert shows the p-values (chi-squared test) of the features. (D) K-means clustering (MCA component 1 and 2 correspond to the first 2 principal components) in the multiple correspondence analysis space. Each oval indicates 1 standard deviation of a 2D gaussian fit.

medRxiv preprint doi: https://doi.org/10.1101/2023.08.06.23293535; this version posted August 9, 2023. The copyright holder for this preprint
(which was not certified by peer review) is the author/funder, who has granted medRxiv a license to display the preprint in perpetuity.
It is made available under a CC-BY-NC-ND 4.0 International license .

We next looked at the importance scores of the different input features, as represented by the sum of the weight values for individual input features across all the layers. We found the largest score for venous outflow stenosis, followed by cortical venous drainage and flow-associated aneurysms. Although there was a certain variability in the score of each attribute between different runs of the algorithm, this importance ranking of outflow stenosis remained consistent.
To verify these findings, we performed a dimensionality reduction by means of multiple correspondence analysis followed by k-means clustering in the dAVF feature vector space. We found that the characters of the fistula that correlate best with the first two components (the eigenvectors with the largest eigenvalue, thus explaining most of the variance in the data) were the architecture of the fistula, venous outflow stenosis, venous ectasia and cortical venous drainage (Figure 2 C). The automatic k-means clustering in this low-dimensional space was verified by checking the agreement between the ground truth (actual outcome) and the cluster labels (adjusted Rand score of 0.273 (range -1 to 1, values closer to 1 indicate better fit), purity index=0.82) (Figure 2 D).

Discussion

Here we describe a novel approach to identify bleeding risk factors for cranial dural arteriovenous fistulas, by revealing patterns and their features in the data that best discriminate hemorrhagic/non-hemorrhagic lesions using MCA coupled with automatic k-means clustering and confirming the relevance of these hidden, important angiographic features that best predict hemorrhage using a shallow artificial neural network. This approach achieved 80% accuracy in correctly classifying those dAVF that present with hemorrhage, and showed the importance of new, previously ignored features such as venous outflow stenosis and angio-architecture of the fistula. Additionally, the machine learning approach confirmed the relevance of previously deemed important characters such as venous ectasia(4, 11, 12). Intriguingly, this analysis suggest, for the first time, that the same characters (venous outflow stenosis) that are associated with increased rupture risk in other, more frequent shunting vascular malformation such as the cerebral arteriovenous malformation (AVM)(13) presumably play the same role in dAVF.
The presence of pial feeding arteries(14) and cortical venous drainage with or without abnormal venous dilatation(6) have been considered independent risk factors for predicting the natural history of dAVF. As such, some of these characters (cortical venous drainage, venous ectasia) are part of the widely used classifications of Borden and Cognard that guide treatment decision(5, 6). Despite the caveats of applying machine learning to small datasets (but see Olson et al., 2018 for a sound argument against this)(15), our work confirms and extends the findings of prior studies and makes the argument that the concomitant presence of these four features on the conventional angiography may be sufficient to achieved greater discrimant power regarding the bleeding risk. To our knowledge this is the first study in literature that applies machine learning in evaluating features of dAVF predictive for hemorrhage risk and is an approach that can be applied to other lesions and organs.

medRxiv preprint doi: https://doi.org/10.1101/2023.08.06.23293535; this version posted August 9, 2023. The copyright holder for this preprint
(which was not certified by peer review) is the author/funder, who has granted medRxiv a license to display the preprint in perpetuity.
It is made available under a CC-BY-NC-ND 4.0 International license .

Conclusions

Using machine learning, we show the importance of two new angiographic features (venous outflow stenosis and fistula architecture) for the evaluation of dAVF's. Their presence, independent or in addition to cortical venous drainage, venous ectasia and pial feeders, can predict with relative high accuracy the hemorrhagic risk of these lesions. This shows that simple machine learning algorithms can identifying potential relevant, hidden, angio-architectural features of dural arteriovenous fistulas helping neurosurgeons and interventional neuroradiologists in the clinical decision-making process. Our approach can be applied to larger and more complex datasets as well to other vascular or non-vascular lesions.

Disclosure. The authors have no competing financial interests.

Data availability statement. Data is available upon reasonable request. The authors confirm that the data used in this study cannot be made available in the manuscript, the online supplemental files or in a public repository due to the German data protection law ("Bundesdatenschutzgesetz", BDSG)

Ethics approval. This study was approved by the Ethics Committee of the Witten/ Herdecke University

ORCID iD's
Mihai Manu: **https://orcid.org/0000-0001-7776-4736**

References

1. Satomi J, Satoh K. [Epidemiology and etiology of dural arteriovenous fistula]. Brain Nerve. 2008;60(8):883-6.
2. Elhammady MS, Ambekar S, Heros RC. Epidemiology, clinical presentation, diagnostic evaluation, and prognosis of cerebral dural arteriovenous fistulas. Handb Clin Neurol. 2017;143:99-105.
3. Ide S, Kiyosue H. [Dural Arteriovenous Fistula]. No Shinkei Geka. 2021;49(2):362-7.
4. Borden JA, Wu JK, Shucart WA. A proposed classification for spinal and cranial dural arteriovenous fistulous malformations and implications for treatment. J Neurosurg. 1995;82(2):166-79.
5. Cognard C, Gobin YP, Pierot L, Bailly AL, Houdart E, Casasco A, et al. Cerebral dural arteriovenous fistulas: clinical and angiographic correlation with a revised classification of venous drainage. Radiology. 1995;194(3):671-80.

medRxiv preprint doi: https://doi.org/10.1101/2023.08.06.23293535; this version posted August 9, 2023. The copyright holder for this preprint
(which was not certified by peer review) is the author/funder, who has granted medRxiv a license to display the preprint in perpetuity.
It is made available under a CC-BY-NC-ND 4.0 International license .

6. Zipfel GJ, Shah MN, Refai D, Dacey RG, Jr., Derdeyn CP. Cranial dural arteriovenous fistulas: modification of angiographic classification scales based on new natural history data. Neurosurg Focus. 2009;26(5):E14.
7. Söderman M, Pavic L, Edner G, Holmin S, Andersson T. Natural history of dural arteriovenous shunts. Stroke. 2008;39(6):1735-9.
8. Strom RG, Botros JA, Refai D, Moran CJ, Cross DT, 3rd, Chicoine MR, et al. Cranial dural arteriovenous fistulae: asymptomatic cortical venous drainage portends less aggressive clinical course. Neurosurgery. 2009;64(2):241-7; discussion 7-8.
9. Halford, M. Prince [Computer software]. https://github.com/MaxHalford/prince (accessed 20 January 2023)
10. Pedregosa F, Varoquaux G, Gramfort A, Michel V, Thirion B, Grisel O, et al. Scikit-learn: Machine learning in Python. the Journal of machine Learning research. 2011;12:2825-30.
11. Brown RD, Jr., Wiebers DO, Nichols DA. Intracranial dural arteriovenous fistulae: angiographic predictors of intracranial hemorrhage and clinical outcome in nonsurgical patients. J Neurosurg. 1994;81(4):531-8.
12. Gross BA, Du R. The natural history of cerebral dural arteriovenous fistulae. Neurosurgery. 2012;71(3):594-602; discussion -3.
13. Chalil A, Raupp EF, Duckwiler GR, Viñuela F, Lownie SP. Hemodynamic and Anatomical Factors in Arteriovenous Malformation Clinical Presentation: 45 Case Studies. Can J Neurol Sci. 2023;50(1):37-43.
14. Osada T, Krings T. Intracranial Dural Arteriovenous Fistulas with Pial Arterial Supply. Neurosurgery. 2019;84(1):104-15.
15. Olson M, Wyner AJ, Berk R. Modern neural networks generalize on small data sets. Proceedings of the 32nd International Conference on Neural Information Processing Systems; Montréal, Canada: Curran Associates Inc.; 2018. p. 3623–32.